Simulated Microgravity Impairs Cardiac Autonomic Neurogenesis from Neural Crest Cells

Konstantinos E. Hatzistergos,[1] Zhijie Jiang,[2] Krystalenia Valasaki,[1]
Lauro M. Takeuchi,[1] Wayne Balkan,[1] Preethi Atluri,[1] Dieter Saur,[3,4] Barbara Seidler,[3,4]
Nicholas Tsinoremas,[2] Darcy L. DiFede,[1] and Joshua M. Hare[1]

Microgravity-induced alterations in the autonomic nervous system (ANS) contribute to derangements in both the mechanical and electrophysiological function of the cardiovascular system, leading to severe symptoms in humans following space travel. Because the ANS forms embryonically from neural crest (NC) progenitors, we hypothesized that microgravity can impair NC-derived cardiac structures. Accordingly, we conducted in vitro simulated microgravity experiments employing NC genetic lineage tracing in mice with $cKit^{CreERT2/+}$, *Isl1nLacZ*, and *Wnt1-Cre* reporter alleles. Inducible fate mapping in adult mouse hearts and pluripotent stem cells (iPSCs) demonstrated reduced $cKit^{CreERT2/+}$-mediated labeling of both NC-derived cardiomyocytes and autonomic neurons ($P < 0.0005$ vs. controls). Whole transcriptome analysis, suggested that this effect was associated with repressed cardiac NC- and upregulated mesoderm-related gene expression profiles, coupled with abnormal bone morphogenetic protein (BMP)/transforming growth factor beta (TGF-β) and Wnt/β-catenin signaling. To separate the manifestations of simulated microgravity on NC versus mesodermal-cardiac derivatives, we conducted *Isl1nLacZ* lineage analyses, which indicated an approximately 3-fold expansion ($P < 0.05$) in mesoderm-derived $Isl-1^+$ pacemaker sinoatrial nodal cells; and an approximately 3-fold reduction ($P < 0.05$) in cardiac NC-derived ANS cells, including sympathetic nerves and $Isl-1^+$ cardiac ganglia. Finally, NC-specific fate mapping with a *Wnt1-Cre* reporter iPSC model of murine NC development confirmed that simulated microgravity directly impacted the in vitro development of cardiac NC progenitors and their contribution to the sympathetic and parasympathetic innervation of the iPSC-derived myocardium. Altogether, these findings reveal an important role for gravity in the development of NCs and their postnatal derivatives, and have important therapeutic implications for human space exploration, providing insights into cellular and molecular mechanisms of microgravity-induced cardiomyopathies/channelopathies.

Keywords: neural crest cells, microgravity, cardiomyopathy, space travel, cardiac autonomic nervous system, pacemaker cells

Introduction

SPACE EXPLORATION IS PHYSICALLY challenging and studies on humans returning from spaceflight, as well as earth-based simulated microgravity and space radiation experiments, have identified numerous hazards associated with low earth orbit and deep space travel [1]. These exposures may pose a risk to cardiovascular health, including, but not limited to, hemodynamic changes and body fluid shifts [2]; loss of myocardial mass [3]; reduced vascular resistance [1,2]; abnormal heart rate variability [4–6]; and orthostatic intoler-ance [5,7,8]. Importantly, increased mortality rates due to cardiovascular disease have also been reported [1].

Although the underlying mechanisms remain unclear and controversial, clinical and experimental data suggest that the detrimental effects of microgravity on cardiovascular health are related at least in part to alterations in the autonomic nervous system (ANS) and conduction systems [4–7,9–12]. The cardiac ANS develops from a migratory population of cells, the neural crest (NC) [13], which we [14–17] and others [13,18–20] have shown to play an important role in the plasticity and pathophysiology of the developing and adult

[1]Interdisciplinary Stem Cell Institute, University of Miami, Miami, Florida.
[2]Center for Computational Sciences, University of Miami, Miller School of Medicine, Miami, Florida.
[3]Department of Medicine II, Klinikum rechts der Isar, Technische Universität München, München, Germany.
[4]German Cancer Research Center (DKFZ) and German Cancer Consortium (DKTK), Heidelberg, Germany.

heart. The cardiac conduction system, which is largely operated by pacemaker cells in the sinoatrial node (SAN), arises instead from cardiac mesoderm progenitors [21]. Importantly, despite their distinct embryonic origins, both NC and SAN lineages are produced under a cardiac regulatory network involving the stage-specific modulation of the bone morphogenetic protein (BMP) and Wnt signaling pathways [13,22,23]. Recent studies indicate that exposure of mouse embryonic stem cells (mESCs) to simulated microgravity [24] or spaceflight [25] significantly alters their capacity to differentiate into cardiogenic and neurogenic cells, through mechanisms that involve altered Wnt and BMP signaling pathways. However, whether the impact of microgravity on cardiovascular health involves abnormalities in the molecular and cellular mechanisms of the ANS and SAN lineages, remains unknown.

Accordingly, we employed simulated microgravity experiments, combined with $cKit^{CreERT2/+}$, $Isl1nLacZ$, and $Wnt1-Cre$ lineage mapping approaches in mice and induced pluripotent stem cell (iPSC) models of cardiogenesis, to study the impact of microgravity on the ANS and SAN lineages.

Materials and Methods

Animals

All animal studies were performed in an AAALAC-approved animal facility at the University of Miami, Miller School of Medicine, and procedures were performed using IACUC-approved protocols according to NIH standards. The $cKit^{CreERT2/+}$, IRG, $Isl1nLacZ$, $Isl1^{MerCreMer}$, $Wnt1-Cre$, and $tdTomato$ mice have been described previously [14,15].

iPSC modeling experiments

The iPSC$^{Kit-Cre}$ and iPSC$^{Wnt1-Cre}$ mouse iPSC lines have been described elsewhere [14,15]. Mouse iPSCs were propagated without feeders on 0.1% gelatin-coated plates (Millipore), with NDiff227 (Clontech), supplemented with 1,000 U/mL LIF (Millipore), 1 μM PD0325901 (Tocris), and 3 μM CHIR99021 (Tocris). For cardiac NC differentiation, iPSCs were resuspended in differentiation medium [IMDM (Thermo), L-glutamine, 20% FBS (Thermo), 0.1 mM nonessential aminoacids, and 0.1 mM 2-mercaptoethanol] at 25,000 cells/mL and aggregated into embryoid bodies (EBs) in the presence of the small molecule BMP antagonist dorsomorphin (2 μM; Tocris), or 100 μg/mL ascorbic acid (Sigma), using the hanging drop method, as described previously [14,15]. To simulate microgravity, day 4 EBs were randomly transferred into 2-mL high-aspect ratio vessels (HARVs), with or without Sephadex microcarrier beads (Sigma), or in 0.1% gelatin-coated six-well plates (Corning), as control. A total of 30 EBs were cultured per HARV or per well. HARVs were attached into a rotary cell suspension culture system (RCCS; Synthecon), and speed was adjusted every other day at 12–20 rpm, as previously described [24]. To induce $cKit^{CreERT2/+}$ recombination, cultures were supplemented every other day with 1 μM (Z)-4-hydroxytamoxifen (Abcam), from day 6 until the end of the experiment. To explore the effect of transitioning into normal gravity, RCCS-grown EBs were collected on day 10 and plated on gelatin-coated six-well plates, until day 21. Medium was exchanged every other day. Quantification of beating and Cre-reporter gene expression were performed as described previously [14,15]. Live-tissue

epifluorescence imaging was performed in an Olympus IX81 fluorescent microscope, as described before [14,15].

Adult lineage tracing and heart tissue culturing

For tamoxifen-inducible lineage tracing of adult c-Kit$^+$ cardiac cells, female $cKit^{CreERT2/+};IRG$ mice (8–12 weeks old) were treated for 3 consecutive days with intraperitoneal injections of tamoxifen, as previously described [15]. For $cKit^{CreERT2/+};IRG$ tissue culture experiments, heart explants were collected from the interventricular septal wall of adult $cKit^{CreERT2/+};IRG$ mice of both sexes (8–12 weeks old) as previously described [14]. Tissues were minced into ~ 2–$3 \, mm^3$ fragments and digested in a solution of DMEM/F12 (Thermo), 20% FBS (Thermo), 1% penicillin/streptomycin (Thermo), and 200 U/mL Collagenase-Type II solution (Worthington) at 37°C. Digested tissue explants were then collected and washed twice with DMEM (Thermo) to remove residual enzyme. Single tissue fragments were then handpicked under sterile conditions with a stereomicroscope and a micropipette, and randomly transferred into six-well plates [static culture (SC)] or 2 mL-HARVs (RCCS), coated with 2.5×10^5 gamma-irradiated mouse embryonic fibroblasts (MEFs; Millipore). According to manufacturer's instructions (Synthecon), all tissue samples cultured in HARVs were supplemented with MEF-coated Sephadex microcarrier beads (Sigma). Samples were fed every other day with DMEM/F12, 15% FBS (HyClone), 1% penicillin/streptomycin (Thermo), 1% β-mercaptoethanol (Thermo), 1,000 U/mL recombinant mouse LIF (Millipore), 100 ng/mL recombinant mouse SCF (PeproTech) 1 ng/mL recombinant mouse bFGF (PeproTech), 0.1 mM nonessential aminoacids (Thermo), and 1 μM (Z)-4-hydroxytamoxifen. Quantification of Cre reporter gene expression in heart explants was performed as described before [14].

For $Isl1nLacZ$ tissue culture experiments, $Isl1nLacZ$ hearts of both sexes (8–12 weeks old) were harvested and rinsed in ice cold Hanks' balanced salt solution (HBSS; Thermo Scientific), before dissecting both ventricles and atria under a stereomicroscope (Discovery V8; Zeiss). The remaining tissue, containing the intact inflow and outflow tracts, the outflow tract base, and sinus node, was cleared from any epicardial fat, esophageal and pharyngeal tissue fragments, and placed in SC with DMEM/F12 (Thermo), 20% FBS (Thermo), 1% penicillin/streptomycin (Thermo), 0.1 mM nonessential aminoacids (Thermo), and 1% β-mercaptoethanol (Thermo), at 37°C/5% CO$_2$. After 1 h, tissues were collected in fresh medium and randomized into SC or RCCS cultures. Medium was changed every 2 days. MEF-coated microcarrier beads were not used in this set of experiments. After a total period of 2 weeks, samples were collected, fixed for 10 min in 4% paraformaldehyde, and processed for X-gal staining as previously described [15]. X-gal-stained samples were subsequently imaged in a Zeiss, Discovery V8 stereomicroscope equipped with a Nikon D7200 digital camera. For X-gal quantification, jpeg images were used to select the X-gal$^+$ areas in Adobe Photoshop Elements (version 12.1) using the semiautomated color range selection tool, and converted into pixel values.

Immunostaining

Confocal immunofluorescence was performed in adult heart tissue and iPSC-derived EBs as previously described

[14,15]. The following antibodies were used: anti-enhanced green fluorescent protein (EGFP) (chicken monoclonal, 1:500; Aves); Nkx2.5 (goat polyclonal, 1:50; Santa Cruz biotechnologies); vesicular acetylcholine transporter (1:200; Novus Biologicals); Tyrosine Hydroxylase (rabbit polyclonal, 1:500; Novus Biologicals), Tuj1 (Rabbit polyclonal, 1:500; Covance). Subsequently, the antibodies were visualized by incubating the cells for 45 min at RT with Alexa 488, Alexa 546, or Alexa 647 secondary antibodies (Molecular probes).

TaqMan gene expression analysis

TaqMan gene expression analysis was performed as described previously [14,15]. Briefly, RNA was isolated from EBs using the RNeasy Plus Mini Kit (Qiagen), according to the manufacturer's instructions. RNA quality was assessed using NanoDrop (Thermo). cDNA was generated using the High-Capacity cDNA Reverse Transcription Kit (Thermo), and gene expression was analyzed using the TaqMan Universal PCR Master Mix (Thermo) in a Bio-Rad Q5 Real-Time PCR. For the analysis, all values were normalized to GAPDH. The following probes were used: Mm99999915_g1, GAPDH; Mm00432087_m1, BMP4; Mm01300555_g1, WNT1; Mm00440359_m1, MYH7; Mm01297833_s1, NOGGIN; Mm00550265_m1, LEF1; Mm00435491_m1, PAX3; Mm01309813_s1, NKX2.5; Mm00445212_m1, CKIT; Mm00486938_m1, CDH5; Mm00443610_m1, AXIN2; Mm0044321_m1, SEMA3C; Mm01224783_m1, SEMA3D; Mm01222421_m1, KDR; Mm00486299_s1, SOX1; Mm00517585_m1, ISL1; Mm00447557_m1, TH; and Mm01221880_m1, CHAT.

Microarray analysis

RNA was collected from ascorbic acid-treated iPSC$^{Kit-Cre}$-derived EBs, on days 10 ($n = 3$ SC and $n = 3$ RCCS) and 21 ($n = 3$ SC and $n = 3$ RCCS), using the RNeasy Plus Mini Kit (Qiagen), according to the manufacturer's instructions. RNA quality was assessed in an Agilent Bioanalyzer, at the University of Miami, Hussman Institute of Human Genomics, Center for Genome Technology (HIHG-CGT), Gene Expression Core Facility. One sample from the day 10 RCCS group failed the quality test and was therefore excluded from the array. A total of $n = 11$ samples were analyzed on the Affymetrix GeneChip Mouse Gene 2.0 ST array, at the HIHG-CGT. Analysis of array data was conducted in R package [26]. The CEL files of 11 samples were read into R and sample quality was evaluated in R before normalization. The normalized data were tested by F-test to remove genes whose expression values are not different among groups. Hierarchical clustering and PCA were applied on filtered gene set to evaluate the relationship among samples. Limma package was used to fit the expression values of four groups, and then the genes of significantly differential expression and adjusted $P < 0.05$ between each two groups were collected. The enrichment analyses on DE genes were conducted in GeneGo (MetaCore Bioinformatics software, Thomson Reuters), and top 10 enriched pathways and gene ontology processes were reported.

Statistics

All statistical analyses, except microarrays, were performed using GraphPad Prism version 5.00 for Windows. Values were analyzed using Student's t-test, Mann–Whitney, or ANOVAs (one- or two-way) followed by Tukey's post hoc tests. All data met the assumptions of the tests. A $P < 0.05$ was considered statistically significant. All values are reported as mean $\pm$ SEM.

Results

Effects of simulated microgravity on adult and iPSC-derived cKit$^+$ cardiac cells

Contrary to the harmful effects of spaceflight in human cardiovascular pathophysiology [1,6], exposure to microgravity exerts beneficial effects on the cardiac mesoderm differentiation of pluripotent stem cell-derived progenitors [24,25].

To address this paradox, we first tested the effect of simulated microgravity on the fate of adult cardiac precursor cells, by combining a RCCS with a $cKit^{CreERT2/+}$; IRG-inducible genetic fate-mapping approach in adult mice, under which the expression of the cell surface marker $cKit$ results in Cre-mediated irreversible replacement of Discosoma sea anemones-derived red fluorescent protein (DSRED) with the EGFP fluorescent reporter gene, upon induction with tamoxifen [14,15]. In agreement with earlier reports [14,15], $cKit^{CreERT2/+}$;IRG fate mapping marked a rare pool of $cKit^+$ cells in the adult heart which contributed to postnatal turnover of cardiomyocytes and autonomic neurons (Fig. 1A–D). To study the responses of adult $cKit^+$ cells to microgravity, myocardial tissue was extracted from the interventricular septum of $cKit^{CreERT2/+}$;IRG adult mice and randomized to be cultured on MEF feeder layers for up to 2 months, either under SC or RCCS conditions, in the presence of 4-hydroxytamoxifen, as described previously [14,23]. Both SC and RCCS cultures promoted the outgrowth of proliferative cardiac cells from within the myocardial explants (Fig. 1E–G). However, although the SC group became enriched in migratory EGFP$^+$ $cKit^+$ cells over time (Fig. 1G, H), there was complete absence of EGFP expression, both within the explanted tissues and in explant-derived cells, in the RCCS group ($P < 0.005$) (Fig. 1E, F, H).

To better understand this observation, we developed an iPSC approach to model cardiac $cKit^+$ cell development and differentiation, by generating iPSCs from $cKit^{CreERT2/+}$;IRG reporter mice (iPSCs$^{Kit-Cre}$) [14,15]. To direct differentiation toward the cardiac lineages, iPSCs$^{Kit-Cre}$ were first aggregated into EBs under SC, in the presence of ascorbate or the BMP antagonist Dorsomorphin (DM) as previously described [14,15]. To genetically fate-map the impact of simulated microgravity on iPSCs$^{Kit-Cre}$-derived $cKit^+$ cells, EBs were randomized onto gelatin-coated plates (SC) or RCCS on EB day 4 and subjected to treatment with 4-hydroxytamoxifen until their full cardiac differentiation on EB day 10. Analysis of EGFP expression and spontaneous contractions on EB day 10, indicated an approximately 5-fold decrease in the rate of spontaneously beating EBs ($P < 0.005$), and an approximately 6-fold decrease in the number of EBs containing EGFP$^+$/Nkx2.5$^+$ derivatives ($P < 0.05$) in RCCS compared with SC (Fig. 2A–H, and Supplementary Movies S1–S2; Supplementary Data are available online at www.liebertpub.com/scd).

Altogether, these findings suggest that, contrary to its beneficial effects on the cardiac mesoderm differentiation of pluripotent stem cells [24,25], simulated microgravity exerts
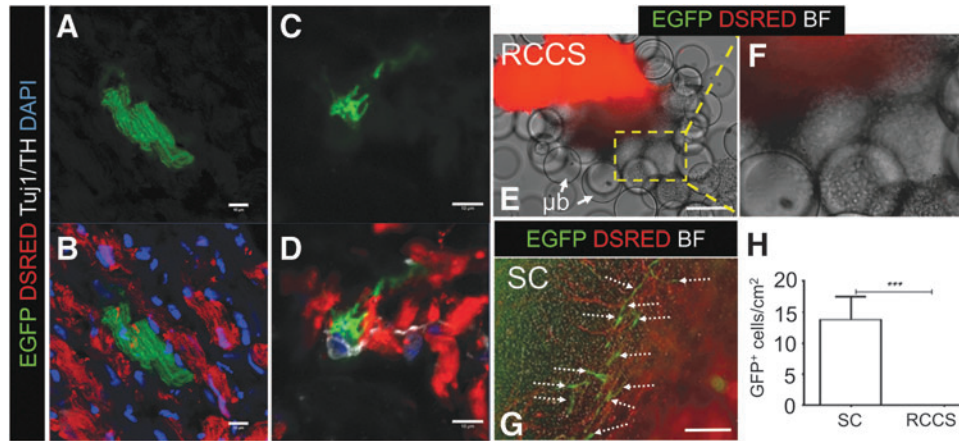
FIG. 1. Rotary Cell Culture System (RCCS) impairs $cKit^+$ cells in the adult heart. **(A–D)** An enhanced green fluorescent protein (EGFP)$^+$ cardiomyocyte **(A–B)** and Tuj1$^+$/TH$^+$ neuron **(C, D)** following 2-week $cKit^{CreERT2/+}$;IRG lineage fate mapping ($n=3$), indicates contribution of adult $cKit^+$ cells to postnatal cardiomyocyte and ANS renewal. **(E, F)** Live tissue imaging of EGFP and Discosoma sea anemone-derived red fluorescent protein (DSRED) in cardiac explants from a $cKit^{CreERT2/+}$;IRG mouse heart, cultured for 24 days in RCCS in the presence of 4-hydroxytamoxifen, illustrates loss of the $cKit$-CreERT2 lineage, as indicated by the lack of EGFP expression in the explant as well as in explant-derived cells (*boxed* region) migrating onto the MEF-coated microbeads (μb). **(F)** Is a higher magnification of the *boxed* region in **(E)**. **(G)** In contrast to RCCS, culture under static (SC) conditions promotes the outgrowth of EGFP$^+$ cardiac explant-derived cells (*arrows*). **(H)** Quantification of EGFP$^+$ cells under SC and RCCS ($n=5$ mice/group). Values are mean±SEM. ***$P<0.0005$. Scale bars 10 μm **(A–D)**, and 150 μm **(E, F)**. ANS, autonomic nervous system; BF, brightfield; MEF, mouse embryonic fibroblast; RCCS, rotary cell suspension culture system; TH, tyrosine hydroxylase.

detrimental effects in both adult and iPSC-derived cardiac $cKit^+$ cells.

Abnormal Wnt and BMP signaling is associated with cKit$^+$ cell defects

To investigate the potential mechanisms underlying the negative effects of simulated microgravity on $cKit^+$ cells, we performed gene expression microarray analysis of day 10 iPSC$^{Kit-Cre}$-derived EBs (Fig. 2A). Overall, a total of 391 genes were found to be differentially expressed between SC and RCCS-grown day 10 EBs (Supplementary Fig. S2 and Supplementary Table S1). More specifically, compared with SC, EBs subjected to RCCS exhibited significant enrichment in cardiogenic mesoderm-related genes, such as *Mef2C, Msx1, Hand2, Kdr, pecam1, and Tbx3* (Supplementary Table S2); whereas, expression of neuroectodermal lineage-related genes, such as *Sox1, Pax3, Sema3C, Sema3D, Sema3E,* and *Zic3* (Supplementary Table S3), were significantly downregulated. Furthermore, enrichment analysis by sorting for the 10 most significantly affected gene networks and gene ontology processes, revealed a significant impact of RCCS on cardiovascular, neurogenic, and epithelial-to-mesenchymal transition gene programs compared
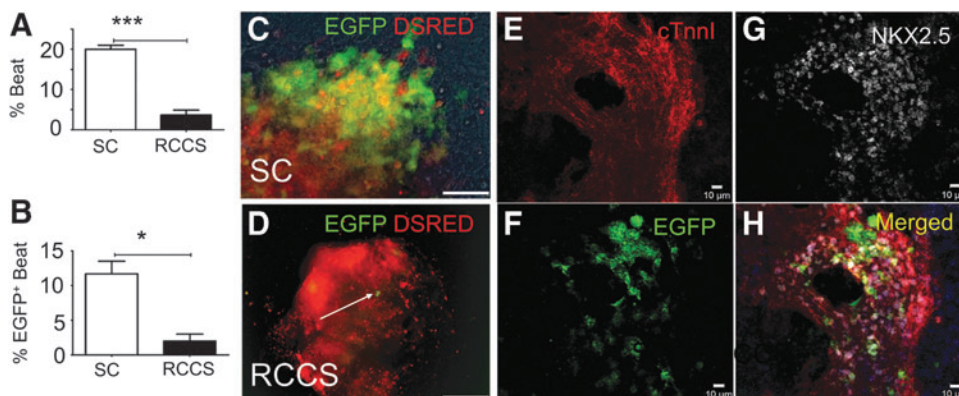

FIG. 2. RCCS impairs embryonic development of $cKit^+$ cells in an iPSC$^{kit-Cre}$ model of cardiogenesis. **(A, B)** Quantification of spontaneously beating EBs **(A)** and spontaneously beating EBs expressing enhanced green fluorescent protein (EGFP) **(B)** under SC or RCCS ($n=3$/group). **(C, D)** Live tissue imaging of EGFP and Discosoma sea anemone-derived red fluorescent protein (DSRED) in SC **(C)** and RCCS-grown **(D)** iPSC$^{kit-Cre}$-derived EBs, following NC differentiation and induction of *Cre*-mediated recombination with 4-hydroxytamoxifen. **(E–H)** Confocal immunofluorescence showing colocalization of EGFP, NKX2.5, and cardiac troponin I in iPSC$^{kit-Cre}$-derived $cKit^+$ NCs, grown under SC. Two-tailed *t*-test, *$P<0.05$, ***$P<0.0005$. Values are mean±SEM. Scale bars 150 μm **(C, D)** and 10 μm **(E–H)**. EBs, embryoid bodies; iPSC, induced pluripotent stem cells; NC, neural crest.
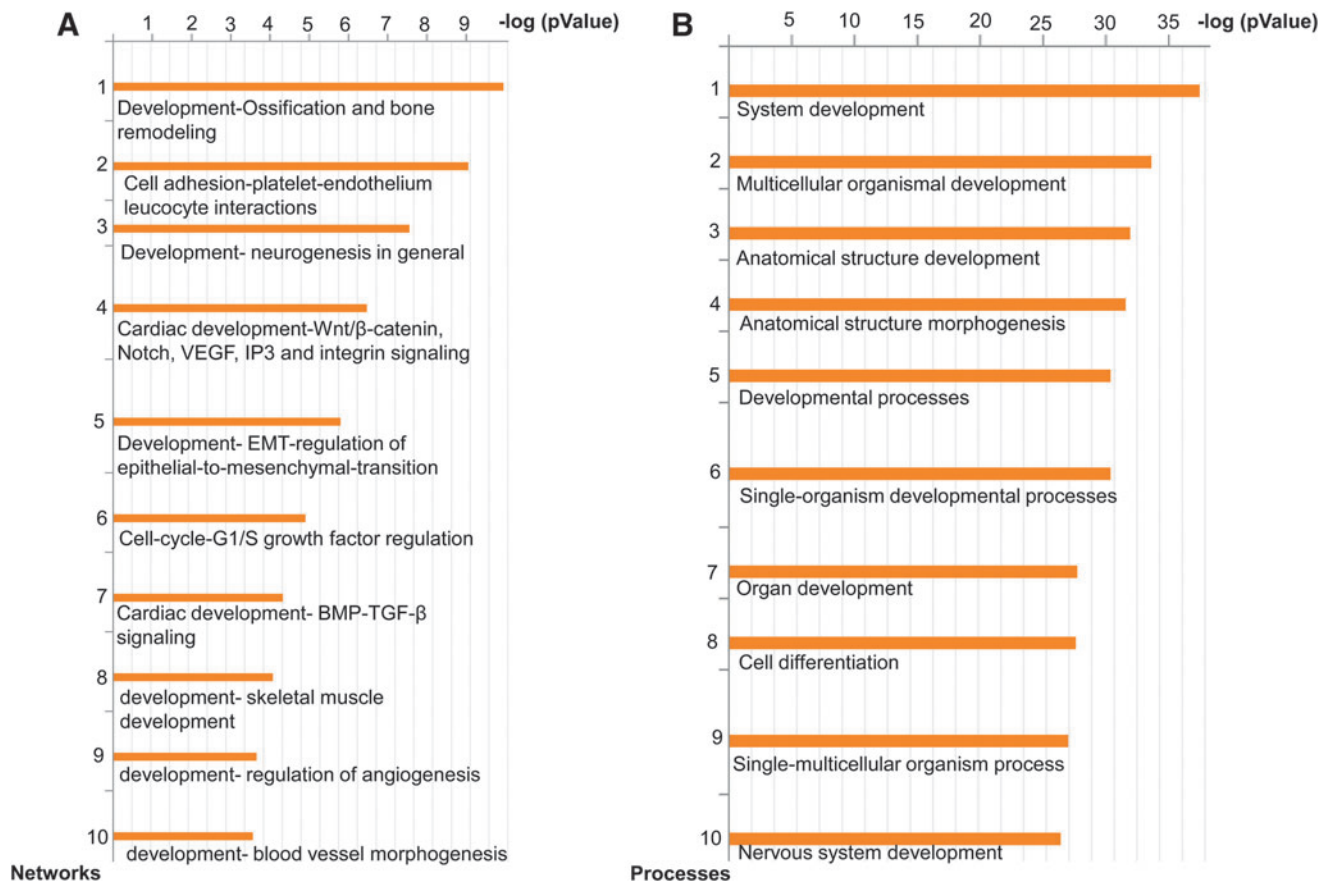
FIG. 3. RCCS affects cardiogenic and neurogenic programs by altering the Wnt and bone morphogenetic protein (BMP) signaling pathways. **(A)** The 10 process networks most significantly affected (statistically significant), based on microarray enrichment analysis of day 10 iPSC$^{kit-Cre}$-derived EBs, grown under SC or RCCS. **(B)** The 10 GO processes most significantly affected, based on microarray enrichment analysis of day 10 iPSC$^{kit-Cre}$-derived EBs, grown under SC or RCCS. ($n = 2$ biological replicates for day 10 RCCS, and $n = 3$ biological replicates for day 10 SC). GO, gene ontology.

with SC; and these effects were accompanied by significant differences in the activities of Wnt/β-catenin and BMP/TGF-β signaling pathways (Fig. 3).

To explore whether the effects of simulated microgravity on cardiac $cKit^+$ cells are reversible, day 10 RCCS iPSC$^{Kit-Cre}$-derived EBs were transferred to SC and subcultured until EB day 21. Microarray analysis indicated a total of 7,337 genes to be differentially expressed between SC and RCCS (Supplementary Fig. S1 and Supplementary Table S4). Enrichment analysis showed that, compared with SC, the abnormalities in the TGF-β/BMP, Wnt/β-catenin, and epithelial-to-mesenchymal transition pathways, persisted in RCCS EBs even after their transfer to SC (Fig. 4A). Moreover, we noted significant differences in gene ontology processes related to biogenesis and organization of subcellular organelles, as well as cell metabolism (Fig. 4B). Notably, similar metabolic abnormalities have been described before on stem cells following actual spaceflight experiments [25].

To verify the microarray results, we performed quantitative polymerase chain reaction (qPCR) analysis. Expression of *Bmp4* and its antagonist *Noggin* corroborated that, compared with SC, the RCCS group was associated with abnormal BMP signaling (Fig. 5A, B). Similarly, differences in *Lef1* and *Axin2* transcription between the two groups corroborated the RCCS-induced abnormalities in Wnt/β-

catenin signaling indicated by the gene expression microarray (Fig. 5C, D).

Analysis of the cardiomyogenic genes, *Myh6* and *Nkx2.5*, did not show significant differences between groups, (Fig. 5E, F). However, compared with SC, the day 10 RCCS group exhibited significantly higher expression of the vasculogenic genes, *Kdr* and *Cdh5*, which remained upregulated following transition to SC (Fig. 5G, H). Interestingly, compared with the SC group, the transcription factor *Isl-1*, which is commonly expressed in mesoderm- and NC- derived cardiac cells, was significantly upregulated in the RCCS group at day 10, but was significantly downregulated by day 21, following transition to SC (Fig. 5I).

Expression of the NC-related genes, *Pax3* and *Wnt1*, were downregulated at day 10 in the RCCS group, but were expressed at similar levels between groups at day 21 (Fig. 5J, K). In contrast, the NC-related genes, *cKit*, *Sema3C*, and *Sema3d*, were also downregulated at day 10 in the RCCS group, but remained repressed throughout the period of the study (Fig. 5L–N). Consequently, analysis of the adrenergic and cholinergic nerve markers, *Tyrosine Hydroxylase* (*Th*) (Fig. 5O) and *Choline Acetyltransferase* (*ChAT*) (Fig. 5P), indicated that sympathetic and parasympathetic neurogenesis, respectively, from NCs were significantly downregulated in the RCCS group compared with SC, both at days 10 and 21 of the study.
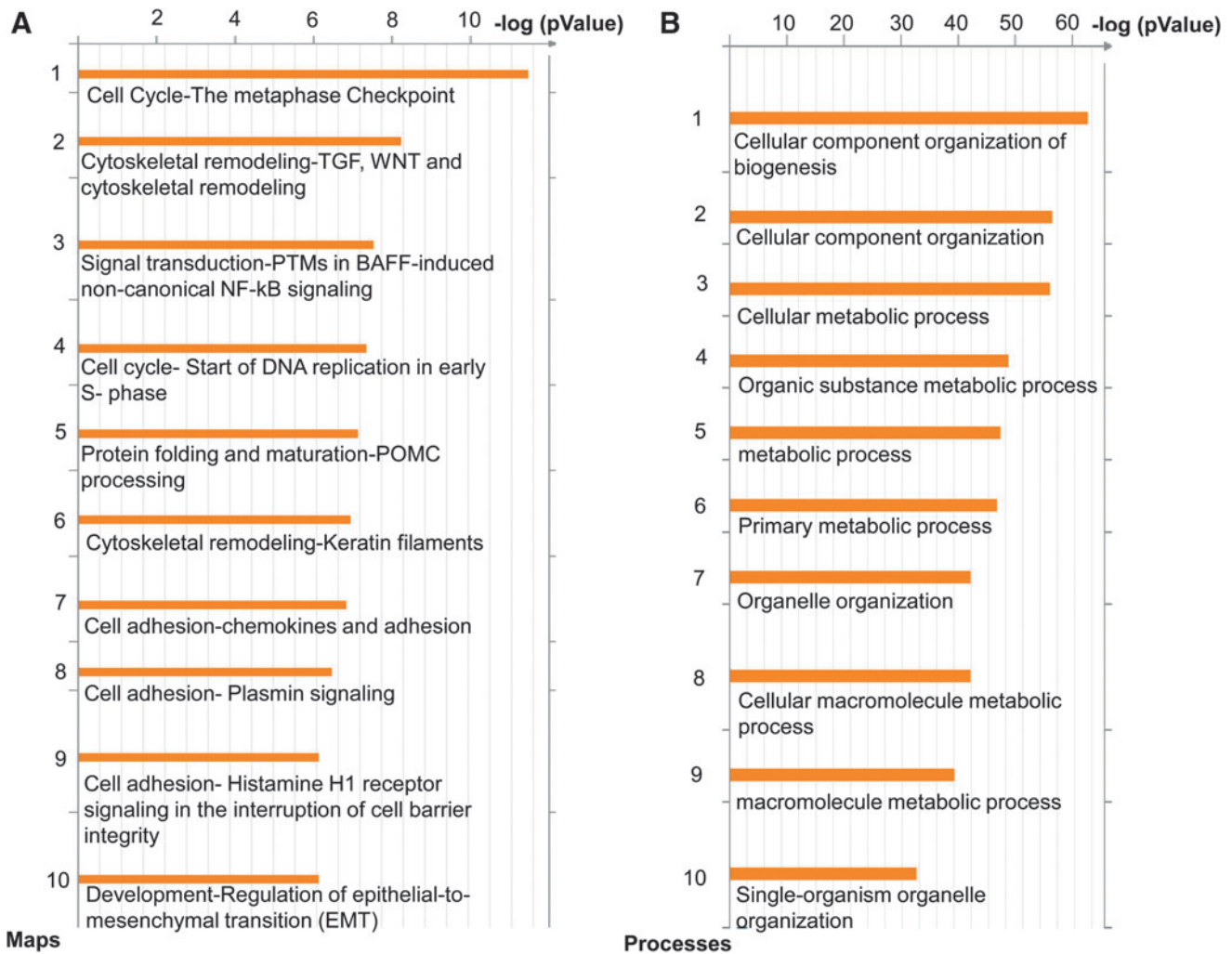
FIG. 4. Abnormal BMP/TGF-β and Wnt/β-catenin following transition from RCCS to SC. **(A)** The 10 signaling pathways most significantly affected based on microarray enrichment analysis of day 21 iPSC$^{kit-Cre}$-derived EBs, grown continuously under SC or following transfer from RCCS to SC on day 10. **(B)** The 10 GO processes most significantly affected, based on microarray enrichment analysis of day 21 iPSC$^{kit-Cre}$-derived EBs, grown continuously under SC or following transfer from RCCS to SC on day 10 ($n = 3$ biological replicates per group).

Collectively, these findings support that the detrimental effects of RCCS on cardiac $cKit^+$ cells are associated with a repressed NC gene expression profile and impaired autonomic neurogenesis, which are not fully reversible upon transition to SC, likely due to underlying abnormalities in Wnt/β-catenin and BMP/TGF-β signaling pathways.

Effects of simulated microgravity on NC versus mesoderm-derived Isl-1$^+$ cardiac cells

The $cKit^{CreERT2/+}$ fate mapping studies suggest that the effects of simulated microgravity are manifested differently between mesoderm and NC-derived cardiac tissues. To test this hypothesis, we investigated the response of postnatal Isl-1$^+$ cardiac cells, which comprise a diverse pool of second heart field (SHF) mesodermal derivatives and NC cells, expressing the ISL LIM homeobox 1 transcription factor Isl-1 [17,27–29].

First, we employed a previously described Isl1nLacZ/+ indicator mouse line [27], to verify the expression of Isl-1 in

postnatal SHF and NC cardiac cells. In agreement with previous reports [17,21,27], X-gal analysis indicated that postnatal Isl1nLacZ expression identifies a group of posterior SHF-derived pacemaker cells in the SAN; a mixed pool of NC- and SHF-derived cells in the proximal outflow tract (OFT); and finally, a group of NC cells in the cardiac ganglia (CGs), located in the dorsal aspect of the heart (Supplementary Fig. S2A). Furthermore, analysis with a tamoxifen-inducible Isl1$^{MerCreMer/+}$ reporter allele [17,27,28] indicated that postnatal Isl-1$^+$ cells retain plasticity and contribute to postnatal turnover of NC-derived sympathetic neurons (Supplementary Fig. S2B), and rarely cardiomyocytes (Supplementary Fig. S2C).

Next, to test the effects of simulated microgravity on postnatal Isl-1$^+$ cells, the cardiac bases of adult Isl1nLacZ mice, which included the SAN, OFT, and CGs, were dissociated from the atria and ventricles and randomized to the SC or RCCS groups. Two weeks later, X-gal analysis indicated that Isl1nLacZ expression in the OFT was similar between the two groups (Fig. 6A, C, E). However, compared
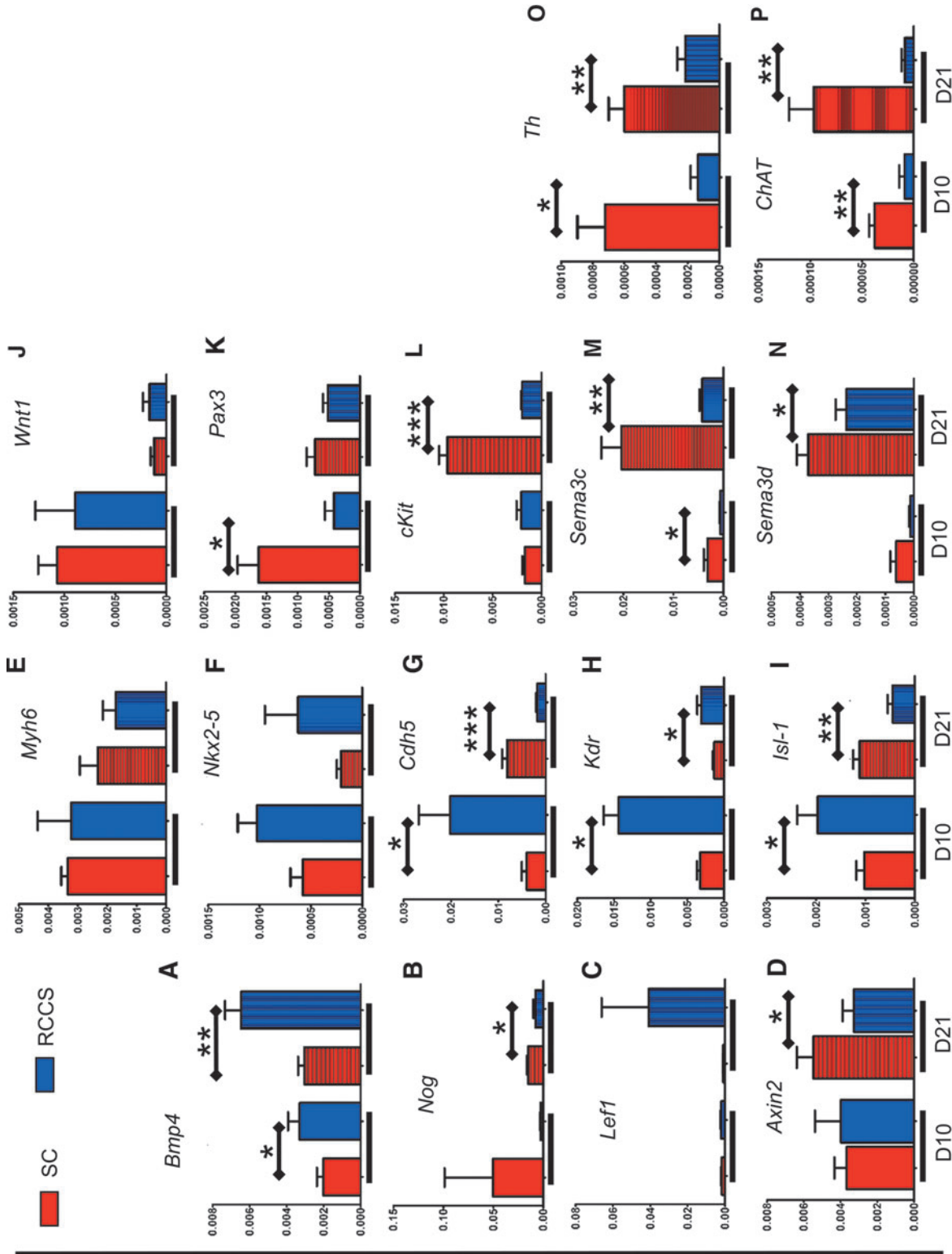
FIG. 5. Impact of RCCS on NC- and cardiogenic mesoderm-related genes. qPCR in NC and cardiogenic mesoderm-related genes found to be differentially expressed between SC and RCCS, at EB days 10 and 21. **(A, B)** RCCS-mediated activation of bone morphogenetic protein (BMP) signaling indicated by upregulated *Bmp4* and downregulated *Noggin* (*Nog*) expression. **(C, D)** RCCS-mediated activation of Wnt signaling indicated by upregulated *Lef1* and downregulated *Axin2* expression. **(E, F)** Comparison of cardiomyogenic genes *Myh6* and *Nkx2-5* between SC and RCCS, before and after transition to SC. **(G, H)** Comparison of vasculogenic genes *Cdh5* and *Kdr* between SC and RCCS, before and after transition to SC. **(I)** Expression of *Isl-1* is upregulated in RCCS at day 10, and downregulated after transition to SC. **(J–N)** Comparison of NC-related genes *Wnt1*, *Pax3*, *cKit*, *Sema3c*, and *Sema3d* between SC and RCCS, before and after transition to SC. **(O, P)** Expression of *Th* and *ChAT* on day 10 and 21 iPSC*^{Kit-Cre}* EBs. (*n* = 2 biological replicates for day 10 RCCS, and *n* = 3 for all other groups). Two-tailed *t*-test, **P* < 0.05, ***P* < 0.005, ****P* < 0.0005. Values are mean ± SEM. qPCR, quantitative polymerase chain reaction.
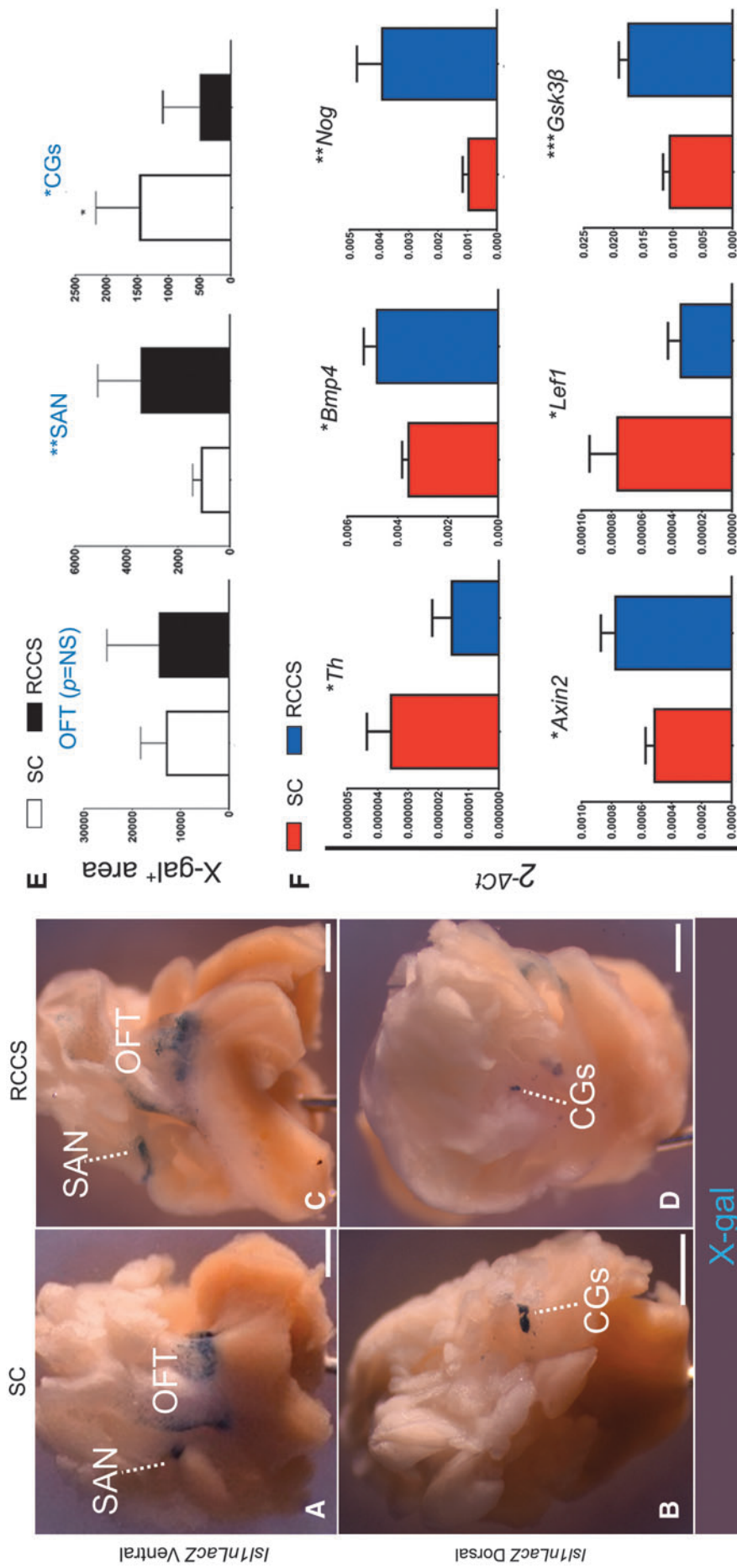
825

FIG. 6. RCCS expands the pool of $Isl1nLacZ^+$ pacemaker cells and reduces the pool of $Isl1nLacZ^+$ ANS cells. (**A, B**) X-gal analysis in $Isl1nLacZ$ adult heart tissues following 2 weeks in SC, indicates that $Isl-1$ is abundantly expressed in sinoatrial node pacemaker cells (**A,** SAN) and the proximal outflow tract (**A,** OFT). Dorsally, $Isl-1$ is abundantly expressed in cardiac ganglia (**B,** CGs). (**C, D**) In contrast, tissues cultured for 2 weeks in RCCS exhibit an expansion of X-gal staining in the SAN (**C**) and diminished X-gal staining in the CGs (**D**). No differences are noted in the proximal outflow tract (**C, D**). (**E**) Quantification of X-gal$^+$area in the OFT, SAN, and CGs, between groups. (**F**) qPCR analysis of $Isl1nLacZ$ adult heart tissues indicates that compared with SC, the RCCS group exhibits reduced sympathetic neurogenesis, as indicated by Th expression. Furthermore, these differences are accompanied by abnormal bone morphogenetic protein (BMP) signaling, as indicated by the expression of $Bmp4$ and $Noggin$ (Nog); as well as abnormal canonical Wnt signaling, as indicated by the expression of $Axin2$, $Lef1$, and $Gsk3\beta$. $n = 5$/group. $*P < 0.05$; $**P < 0.005$; $***P < 0.0005$, two-tailed T-test. Values are mean±SEM. Scale bars 5 mm.
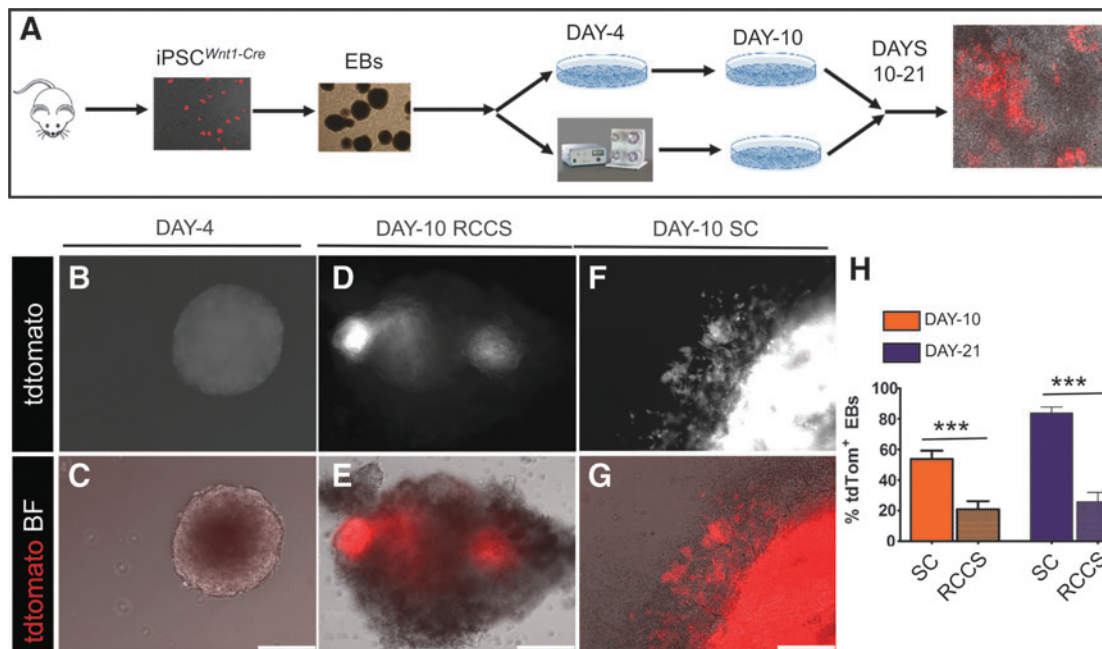
FIG. 7. RCCS specifically compromises NC lineage development. **(A)** Schematic of the iPSCs$^{Wnt1-Cre}$ model of microgravity-induced cardiomyopathy. **(B, C)** Live epifluorescence imaging demonstrating absence of tdTomato expression in day 4 iPSC$^{Wnt1-Cre}$ EBs, immediately before transfer to RCCS, indicating that NC differentiation has not commenced. **(D–G)** tdTomato expression in day 10 iPSC$^{Wnt1-Cre}$ EBs, indicative of NC differentiation. Expression of tdTomato is less abundant in RCCS- **(D, E)** than SC-grown **(F, G)** EBs. **(H)** Quantification of tdTomato epifluorescence under RCCS and SC on day 10; and day 21, after transition on day 10 EBs from SC to RCCS ($n = 17$/group at day 10; $n = 7$ for RCCS on day 21; $n = 12$ for SC at day 21). ***$P < 0.0001$, two-tailed T-test. Values are mean ± SEM. Scale bars 150 μm.

with SC, the RCCS group displayed an approximately 3-fold expansion ($P < 0.05$) in the pool of X-gal$^+$ pacemaker cells in the SAN (Fig. 6A, C, E), and an approximately 3-fold reduction ($P < 0.05$) in the pool of X-gal$^+$ cells in the CGs (Fig. 6B, D, E). Furthermore, qPCR analysis indicated that these manifestations were accompanied by a significant reduction in the expression of the sympathetic nerve marker *Th* (Fig. 6F); and more importantly, by abnormalities in BMP signaling as indicated by differences in *Bmp4* and *Noggin* expression (Fig. 6F) and Wnt/β-catenin signaling, as indicated by differences in *Axin2*, *Lef1*, and *Gsk3β* expression (Fig. 6F).

Taken together, these findings suggest that RCCS-induced abnormalities in Wnt and BMP signaling are manifested as a significant expansion of posterior SHF-derived *Isl-1$^+$* conduction system cells in the SAN; and repression of NC-derived ANS cells, including sympathetic nerves and *Isl-1$^+$* CGs.

Effects of simulated microgravity on iPSCs-derived cardiac NC cells and ANS

Although the experiments with the *cKit* and *Isl-1* alleles support the hypothesis that simulated microgravity induces NC-based abnormalities of the ANS, neither *cKit* or *Isl-1* are NC-specific markers. Accordingly, we sought to specifically test the effects of simulated microgravity on cardiac NCs, by generating a NC-specific *Cre*-reporter iPSC line (iPSC$^{Wnt1-Cre}$) from *Wnt1-Cre;tdTomato* neonatal mouse cardiac fibroblasts [15].

As with the iPSCs$^{Kit-Cre}$, iPSC$^{Wnt1-Cre}$ were differentiated into EBs before being transferred into SC or RCCS on day

4, for up to 21 days (Fig. 7A). By day 9, a migratory population of tdTomato$^+$ cells emerged from within the iPSC$^{Wnt1-Cre}$ EBs, indicating differentiation into NC cells (Fig. 7B, C). Quantification of tdTomato$^+$ EBs on day 10 indicated that NC differentiation was significantly impaired in the RCCS group compared with SC ($20.8\% \pm 5.3\%$ vs. $53.7\% \pm 5.5\%$ tdTomato$^+$ EBs in RCCS and SC groups, respectively, $P < 0.0001$) (Fig. 7D–H)].

To test whether the RCCS-induced defects in NC development can be rescued following transition to SC, iPSCs$^{Wnt1-Cre}$-derived EBs were transitioned from RCCS to SC on day 10, and subcultured until EB day 21. However, tdTomato quantification indicated that the degree of NC differentiation was still significantly lower in the RCCS group compared with SC ($25.7\% \pm 6.1\%$ vs. $83.8\% \pm 3.8\%$ tdTomato$^+$ EBs at day 21, between RCCS and SC groups, respectively; $P < 0.0001$) (Fig. 7H).

Live-cell imaging and confocal immunofluorescence did not show any differences in the capacity of iPSCs$^{Wnt1-Cre}$-derived tdTomato$^+$ NCs to differentiate into NKX2.5$^+$ spontaneously beating cardiomyocytes (Fig. 8A–C and Supplementary Movies S3–S4). However, although tdTomato$^+$ NCs in the SC group contributed extensively to the cardiac autonomic innervation of spontaneously beating EBs with tdTomato$^+$ sympathetic and parasympathetic nerves (Fig. 8D–F, J–L, and Supplementary Movie S5), differentiation of iPSCs$^{Wnt1-Cre}$-derived NCs into cardiac ANS derivatives was diminished in the RCCS group (Fig. 8A–C, G–I, and Supplementary Movie S6).

Collectively, these findings indicate that RCCS directly impacts the development of the NC lineage from iPSCs, and
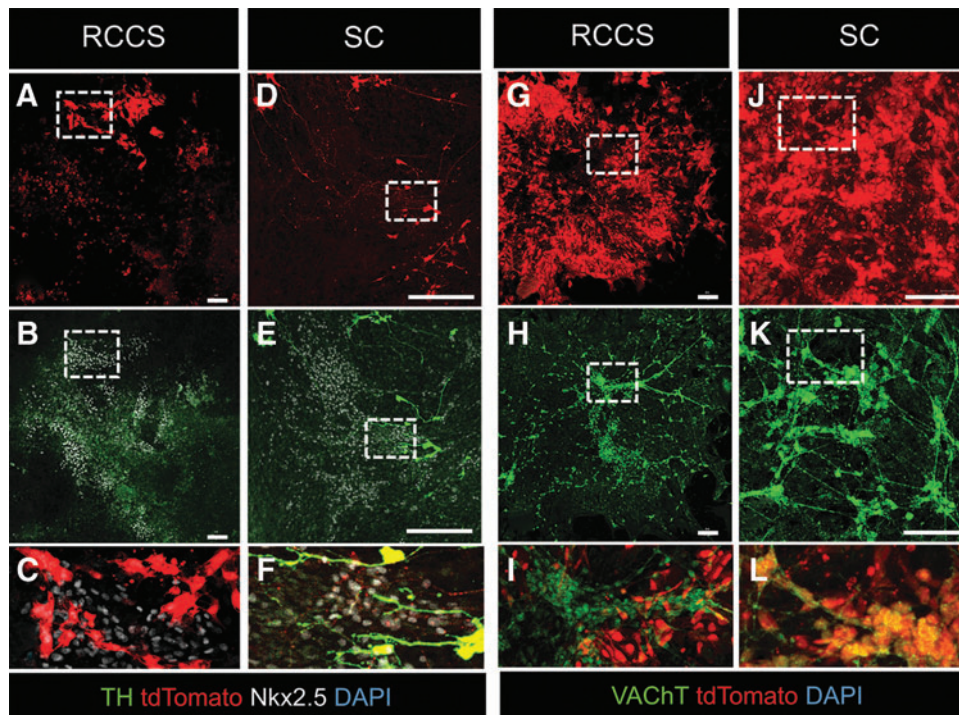
FIG. 8. RCCS compromises NC differentiation into cardiac ANS. **(A–F)** Confocal immunofluorescence of TH, Nkx2.5, and tdTomato on day 19 iPSC$^{Wnt1-Cre}$ EBs, transitioned from RCCS on day 10 **(A–C)** or continuously grown in SC **(D–F)**. Exposure to RCCS supports differentiation of EBs into tdTomato$^+$/Nkx2.5$^+$ myocardium, which however lacks sympathetic innervation, as indicated by the complete lack of TH$^+$ neurons **(A–C)**. In contrast, SC-differentiated Nkx2.5$^+$ myocardium is innervated with tdTomato$^+$/TH$^+$ sympathetic neurons **(D–F)**. **(C, F)** Are blownup images of the areas depicted in *insets* in **(A, B, D, E)**, respectively. **(G, H)** Confocal immunofluorescence of vesicular acetylcholine transporter (VAChT) and tdTomato on day 19 iPSC$^{Wnt1-Cre}$ EBs, transitioned from RCCS on day 10 **(G–I)** or continuously grown in SC **(J–L)**. Exposure to RCCS results in EB differentiation into VAChT$^+$/tdTomato-negative parasympathetic neurons **(G–I)**. In contrast, parasympathetic neurons in SC-differentiated EBs are derived from NCs, as indicated by colocalization of tdTomato$^+$/VAChT$^+$ **(J–L)**. **(I, L)** Are higher magnification images of the areas depicted in *insets* in **(G, H, J, K)**, respectively. Scale bars 100 μm.

consequently, their contribution to sympathetic and parasympathetic innervation of iPSC-derived myocardium; and further suggest that these defects may not be fully reversible upon transition to SC.

Discussion

We employed a series of earth-based in vitro experiments to separate the effects of microgravity on NC versus mesodermal cardiac precursors. The major new finding of this study is that simulated microgravity exerts adverse effects on the autonomic and pacemaking pathways of the heart, by directly repressing NC while enhancing mesoderm-derived cardiac lineages (Supplementary Fig. S3). More specifically, we found that simulated microgravity produced perturbations in the expression of $cKit^{CreERT2/+}$, $Isl1nLacZ$, and $Wnt1$-Cre reporter alleles in adult as well as iPSC-derived cardiac NCs and ANS derivatives, whereas promoting the expansion of $Isl1nLacZ$ reporter gene expression in SHF-derived pacemaker cells of the sinus node. Furthermore, gene expression microarrays and qPCR analyses suggested that these effects were associated with abnormalities in BMP/TGF-β and Wnt/β-catenin signaling; and may not be fully reversible upon transition to normal gravity.

In agreement with our findings, microgravity-induced abnormalities associated with the cardiac ANS and SAN have been previously reported in humans subjected to spaceflight [2,3,5,6,10,11,30–33]. Particularly, transition to microgravity has been reported to induce cardiovascular deconditioning, an acute syndrome manifested as abnormal cardiac preload, stroke volume, and output; loss of myocardial mass; reduced vascular resistance; abnormal baroreflex responses; heart rate variability; and orthostatic intolerance [4–7,11]. Furthermore, a retrospective analysis recently reported significantly higher mortality rates of the Apollo lunar astronauts due to cardiovascular disease [1]. Importantly—although the etiologies for the disease remain undetermined—in support to our study, a cohort of the lunar astronauts reportedly experienced unstable autonomic nervous function and cardiac rhythm problems, including bigeminy as well as premature auricular and ventricular contractions, both during and after space travel [12,34]. Thus, the detrimental effects of microgravity in postnatal cardiac NCs and their ANS derivatives, in conjunction to the abnormal expansion of $Isl-1^+$ conduction system cells in the SAN described in this study, provide a possible explanation for the development of spaceflight-induced cardiomyopathies in humans.

Our findings on simulated microgravity-induced abnormalities in adult and iPSC-derived NC cells are also in agreement with previous developmental studies, reporting neural tube and other neurological defects in urodeles [35,36] and rodents [37,38] in response to actual spaceflight. In addition, consistent with our findings that these effects were associated with abnormal BMP/TGF-β and Wnt/β-catenin signaling, Lei et al. reported enhanced mesendoderm and repressed neuroectodermal differentiation of mESCs in RCCS, due to increased expression of Wnt3 [24]. Similarly, Blaber et al. recently investigated the effects of microgravity during spaceflight on mESCs, and reported abnormalities in several signaling pathways, including Wnt/β-catenin and TGF-β/BMP [25]. Remarkably, compared with our findings and previous simulated microgravity experiments by others [24], the effects of spaceflight on mESCs were associated with retention of pluripotency and inhibition of differentiation into both mesendodermal and neuroectodermal lineages, suggesting that earth-based simulated microgravity experiments may not recapitulate the full spectrum of spaceflight-induced abnormalities on stem/progenitor cells.

Finally, several limitations should be taken into account when interpreting our findings. First, the data described in this study are derived from earth-based simulated microgravity experiments. Second, the impact of simulated microgravity in cardiovascular development and plasticity were assessed ex vivo, in explanted heart tissues and iPSC-based in vitro models of cardiogenesis. Third, our experiments were conducted in murine tissues and cell lines. Therefore, further studies are warranted to elucidate whether the NC-based molecular and cellular mechanisms described herein, are associated with microgravity-induced cardiovascular disorders in humans following space travel.

In summary, we employed a series of earth-based experiments to simulate and study the impact of microgravity on the cellular and molecular mechanisms underlying the embryonic development and postnatal plasticity of the mammalian heart. Our findings support that microgravity impacts cardiac NC cells and their ANS derivatives, as well as the cardiac conduction system, by altering the BMP/TGF-β and Wnt/β-catenin signaling pathways. Taken together, our study provides novel mechanistic insights on the effects of microgravity in cardiovascular development and health; and therefore may lead to novel therapeutic strategies for the prevention and treatment of microgravity-induced cardiomyopathies.

Acknowledgments

Author Disclosure Statement

References

1. Delp MD, JM Charvat, CL Limoli, RK Globus and P Ghosh. (2016). Apollo lunar astronauts show higher cardiovascular disease mortality: possible deep space radiation effects on the vascular endothelium. Sci Rep 6:29901.
2. Norsk P, A Asmar, M Damgaard and NJ Christensen. (2015). Fluid shifts, vasodilatation and ambulatory blood pressure reduction during long duration spaceflight. J Physiol 593:573–584.
3. Perhonen MA, F Franco, LD Lane, JC Buckey, CG Blomqvist, JE Zerwekh, RM Peshock, PT Weatherall and BD Levine. (2001). Cardiac atrophy after bed rest and spaceflight. J Appl Physiol (1985) 91:645–653.
4. Liu J, Y Li, B Verheyden, S Chen, Z Chen, Y Gai, J Liu, J Gao, Q Xie, et al. (2015). Is autonomic modulation different between European and Chinese astronauts? PLoS One 10:e0120920.
5. Vandeput S, D Widjaja, AE Aubert and S Van Huffel. (2013). Adaptation of autonomic heart rate regulation in astronauts after spaceflight. Med Sci Monit 19:9–17.
6. Otsuka K, G Cornelissen, Y Kubo, M Hayashi, N Yamamoto, K Shibata, T Aiba, S Furukawa, H Ohshima and C Mukai. (2015). Intrinsic cardiovascular autonomic regulatory system of astronauts exposed long-term to microgravity in space: observational study. Npj Microgravity 1:15018.
7. Mandsager KT, D Robertson and A Diedrich. (2015). The function of the autonomic nervous system during spaceflight. Clin Auton Res 25:141–151.
8. Jung AS, R Harrison, KH Lee, J Genut, D Nyhan, EM Brooks-Asplund, AA Shoukas, JM Hare and DE Berkowitz. (2005). Simulated microgravity produces attenuated baroreflex-mediated pressor, chronotropic, and inotropic responses in mice. Am J Physiol Heart Circ Physiol 289: H600–H607.
9. Anzai T, MA Frey and A Nogami. (2014). Cardiac arrhythmias during long-duration spaceflights. J Arrhythm 30:139–149.
10. Baevsky RM, VM Baranov, Funtova, II, A Diedrich, AV Pashenko, AG Chernikova, J Drescher, J Jordan and J Tank. (2007). Autonomic cardiovascular and respiratory control during prolonged spaceflights aboard the International Space Station. J Appl Physiol (1985) 103:156–161.
11. Arzeno NM, MB Stenger, JJ Bloomberg and SH Platts. (2013). Spaceflight-induced cardiovascular changes and recovery during NASA's Functional Task Test. Acta Astronautica 92:10–14.
12. Rowe WJ. (1998). The Apollo 15 space syndrome. Circulation 97:119–120.
13. Hasan W. (2013). Autonomic cardiac innervation: development and adult plasticity. Organogenesis 9:176–193.
14. Hatzistergos KE, D Saur, B Seidler, W Balkan, M Breton, K Valasaki, LM Takeuchi, AM Landin, A Khan and JM

Hare. (2016). Stimulatory effects of MSCs on cKit+ cardiac stem cells are mediated by SDF1/CXCR4 and SCF/cKit signaling pathways. Circ Res 119:921–930.

15. Hatzistergos KE, LM Takeuchi, D Saur, B Seidler, SM Dymecki, JJ Mai, IA White, W Balkan, RM Kanashiro-Takeuchi, AV Schally and JM Hare. (2015). cKit+ cardiac progenitors of neural crest origin. Proc Natl Acad Sci U S A 112:13051–13056.

16. White IA, J Gordon, W Balkan and JM Hare. (2015). Sympathetic reinnervation is required for mammalian cardiac regeneration. Circ Res 117:990–994.

17. Hatzistergos KE and JM Hare. (2016). Abstract 322: Postnatal Islet-1 cardioblasts are of neural crest and not second heart-field lineage. Circ Res 119:A322–A322.

18. Kimura K, M Ieda and K Fukuda. (2012). Development, maturation, and transdifferentiation of cardiac sympathetic nerves. Circ Res 110:325–336.

19. Tamura Y, K Matsumura, M Sano, H Tabata, K Kimura, M Ieda, T Arai, Y Ohno, H Kanazawa, et al. (2011). Neural crest-derived stem cells migrate and differentiate into cardiomyocytes after myocardial infarction. Arterioscler Thromb Vasc Biol 31:582–589.

20. Tomita Y, K Matsumura, Y Wakamatsu, Y Matsuzaki, I Shibuya, H Kawaguchi, M Ieda, S Kanakubo, T Shimazaki, et al. (2005). Cardiac neural crest cells contribute to the dormant multipotent stem cell in the mammalian heart. J Cell Biol 170:1135–1146.

21. Liang X, G Wang, L Lin, J Lowe, Q Zhang, L Bu, Y Chen, J Chen, Y Sun and SM Evans. (2013). HCN4 dynamically marks the first heart field and conduction system precursors. Circ Res 113:399–407.

22. Brade T, LS Pane, A Moretti, KR Chien and KL Laugwitz. (2013). Embryonic heart progenitors and cardiogenesis. Cold Spring Harb Perspect Med 3:a013847.

23. Mohan R, B Boukens and V Christoffels. (2017). Lineages of the Cardiac Conduction System. J Cardiovasc Dev Dis 4:5.

24. Lei X, Z Deng, H Zhang, H Zhao, J Zhou, S Liu, Q Chen, L Ning, Y Cao, et al. (2014). Rotary suspension culture enhances mesendoderm differentiation of embryonic stem cells through modulation of Wnt/beta-catenin pathway. Stem Cell Rev 10:526–538.

25. Blaber EA, H Finkelstein, N Dvorochkin, KY Sato, R Yousuf, BP Burns, RK Globus and EA Almeida. (2015). Microgravity reduces the differentiation and regenerative potential of embryonic stem cells. Stem Cells Dev 24: 2605–2621.

26. R Development Core Team. (2008). *R: A Language and Environment for Statistical Computing*. R Foundation for Statistical Computing, Vienna, Austria.

27. Sun Y, X Liang, N Najafi, M Cass, L Lin, CL Cai, J Chen and SM Evans. (2007). Islet 1 is expressed in distinct cardiovascular lineages, including pacemaker and coronary vascular cells. Dev Biol 304:286–296.

28. Laugwitz KL, A Moretti, J Lam, P Gruber, Y Chen, S Woodard, LZ Lin, CL Cai, MM Lu, et al. (2005). Postnatal isl1+ cardioblasts enter fully differentiated cardiomyocyte lineages. Nature 433:647–653.

29. Engleka KA, LJ Manderfield, RD Brust, L Li, A Cohen, SM Dymecki and JA Epstein. (2012). Islet1 derivatives in the heart are of both neural crest and second heart field origin. Circ Res 110:922–926.

30. Lees PJ. (2005). Cardiology in space. Hellenic J Cardiol 46: 320–323.

31. White RJ and M Averner. (2001). Humans in space. Nature 409:1115–1118.

32. Leguay G and A Seigneuric. (1981). Cardiac arrhythmias in space. Role of vagotonia. Acta Astronaut 8:795–801.

33. Charles JB, MA Frey, JM Fritsch-Yelle and GW Fortner. (1996). Chapter 3. cardiovascular and cardiorespiratory function. In: *Space Biology and Medicine—Volume III Books 1 & 2—Humans in Spaceflight*. American Institute of Aeronautics and Astronautics, Inc. Reston, Virginia, pp 63–88.

34. Johnston RS, LF Dietlein and CA Berry. *Biomedical Results of Apollo*. (1975). Scientific and Technical Information Office, National Aeronautics and Space Administration: for sale by the Supt. of Docs., U.S. Govt. Print. Off., Washington.

35. Gualandris-Parisot L, D Husson, F Foulquier, P Kan, J Davet, C Aimar, C Dournon and AM Duprat. (2001). Pleurodeles waltl, amphibian, Urodele, is a suitable biological model for embryological and physiological space experiments on a vertebrate. Adv Space Res 28: 569–578.

36. Gualandris-Parisot L, D Husson, A Bautz, D Durand, P Kan, C Aimar, H Membre, AM Duprat and C Dournon. (2002). Effects of space environment on embryonic growth up to hatching of salamander eggs fertilized and developed during orbital flights. Biol Sci Space 16:3–11.

37. Jamon M. (2014). The development of vestibular system and related functions in mammals: impact of gravity. Front Integr Neurosci 8:11.

38. Ronca AE, B Fritzsch, LL Bruce and JR Alberts. (2008). Orbital spaceflight during pregnancy shapes function of mammalian vestibular system. Behav Neurosci 122: 224–232.

Address correspondence to:
Dr. Joshua M. Hare
Interdisciplinary Stem Cell Institute
University of Miami
Biomedical Research Building, Room 909
1501 NW 10th Avenue
Miami, FL 33136

E-mail: jhare@med.miami.edu